Molecular Genetics and Metabolism 119 (2016) 270–277

Contents lists available at ScienceDirect

Molecular Genetics and Metabolism

journal homepage: www.elsevier.com/locate/ymgme

CRISPR-Cas9 induced mutations along de novo purine synthesis in HeLa cells result in accumulation of individual enzyme substrates and affect purinosome formation

Veronika Baresova [1], Matyas Krijt [1], Vaclava Skopova, Olga Souckova, Stanislav Kmoch, Marie Zikanova *

Institute of Inherited Metabolic Disorders, First Faculty of Medicine, Charles University in Prague, General University Hospital in Prague, Ke Karlovu 2, 128 08 Praha 2, Czech Republic

ARTICLE INFO

Article history:
Received 15 June 2016
Received in revised form 19 August 2016
Accepted 19 August 2016
Available online 24 August 2016

Keywords:
De novo purine synthesis
Adenylosuccinate lyase deficiency
AICA-ribosiduria
CRISPR
Human cellular model
Purinosome

ABSTRACT

Purines are essential molecules for nucleic acid synthesis and are the most common carriers of chemical energy in all living organisms. The cellular pool of purines is maintained by the balance between their de novo synthesis (DNPS), recycling and degradation. DNPS includes ten reactions catalysed by six enzymes. To date, two genetically determined disorders of DNPS enzymes have been described, and the existence of other defects manifested by neurological symptoms and the accumulation of DNPS intermediates in bodily fluids is highly presumable.

In the current study, we prepared specific recombinant DNPS enzymes and used them for the biochemical preparation of their commercially unavailable substrates. These compounds were used as standards for the development and validation of quantitative liquid chromatography-tandem mass spectrometry (LC-MS/MS). To simulate manifestations of known and putative defects of DNPS we prepared CRISPR-Cas9 genome-edited HeLa cells deficient for the individual steps of DNPS (CR-cells), assessed the substrates accumulation in cell lysates and growth media and tested how the mutations affect assembly of the purinosome, the multi-enzyme complex of DNPS enzymes. In all model cell lines with the exception of one, an accumulation of the substrate(s) for the knocked out enzyme was identified. The ability to form the purinosome was reduced.

We conclude that LC-MS/MS analysis of the dephosphorylated substrates of DNPS enzymes in bodily fluids is applicable in the selective screening of the known and putative DNPS disorders. This approach should be considered in affected individuals with neurological and neuromuscular manifestations of unknown aetiology. Prepared in vitro human model systems can serve in various studies that aim to provide a better characterization and understanding of physiology and pathology of DNPS, to study the role of each DNPS protein in the purinosome formation and represent an interesting way for the screening of potential therapeutic agents.

1. Introduction

Purines comprise essential molecules for nucleic acid synthesis and are the most common carriers of chemical energy in all living organisms. The cellular pool of purines is maintained by the balance between their de novo synthesis (DNPS), recycling and degradation. DNPS includes ten reactions catalysed by six enzymes (Fig. 1). To date, two genetically determined defects of DNPS have been identified, including the adenylosuccinate lyase (ADSL, EC 4.3.2.2) deficiency (OMIM 103050) [1] and AICA-ribosiduria (OMIM 608688) [2]; both defects

Abbreviations: ADSL, adenylosuccinate lyase; AICAR, aminoimidazolecarboxamide ribotide; AICAr, aminoimidazolecarboxamide riboside; AIR, aminoimidazole ribotide; AIr, aminoimidazole riboside; AMP, adenosine monophosphate; ATIC, bifunctional enzyme 5-aminoimidazole-4-carboxamide ribonucleotide transformylase/inosine monophosphate cyclohydrolase; CAIR, carboxyaminoimidazole ribotide; CAIr, carboxyaminoimidazole riboside; CHO, Chinese hamster ovarian cells; CIP, calf intestinal alkaline phosphatase; CRISPR, clustered regularly interspaced short palindromic repeats; DMEM, Dulbecco's minimum essential medium; DNPS, de novo purine synthesis; FAICAR, formylaminoimidazolecarboxamide ribotide; FGAM, formylglycineamidine ribotide; FGAR, formylglycineamide ribotide; FGAr, formylglycineamide riboside; GAR, glycineamide ribotide; GART, trifunctional enzyme glycinamide ribonucleotide synthetase/aminoimidazole ribonucleotide synthetase/glycinamide ribonucleotide transformylase; HPLC-DAD, high performance liquid chromatography with diode-array detection; LC-MS/MS, liquid chromatography-tandem mass spectrometry; MBP, maltose binding protein; N^{10}-formyl-THF, N^{10}-formyl-tetrahydrofolate; PAICS, bifunctional enzyme phosphoribosylaminoimidazole carboxylase/phosphoribosylaminoimidazole succinocarboxamide synthetase; PFAS, phosphoribosylformylglycinamidine synthetase; PPAT, phosphoribosyl pyrophosphate amidotransferase; PRA, phosphoribosyl amine; PRPP, phosphoribosyl pyrophosphate; SAICAR, succinylaminoimidazolecarboxamide ribotide; SAICAr, succinylaminoimidazolecarboxamide riboside; S-Ado, succinyladenosine; SAMP, succinyladenosine monophosphate.

* Corresponding author at: Institute of Inherited Metabolic Disorders, Ke Karlovu 2, 128 08 Prague 2, Czech Republic.
E-mail address: mzika@lf1.cuni.cz (M. Zikanova).

[1] These two authors contributed to the work equally.

http://dx.doi.org/10.1016/j.ymgme.2016.08.004
1096-7192/

are accompanied by serious neurological involvement and are caused by missense mutations in the *ADSL* and *ATIC* genes, respectively. Defects in the other four genes have not been identified.

The range of the genetic variabilities and allele frequencies available in the Exome Aggregation Consortium (ExAc) database indicate that similar to the *ADSL* and *ATIC* genes, there is (with the exception of the *PPAT* gene) no evolutionary constraints against loss of function or missense mutations in other DNPS genes *GART*, *PFAS* and *PAICS* (Supplementary data 1). Thus, it may be expected that individuals with biallelic mutations in these genes should exist and, similar to the other DNPS defects, may manifest nonspecific neurological and neuromuscular symptoms and the accumulation of specific DNPS intermediates in bodily fluids.

The main limitation regarding the diagnosis of these defects is the absence of a method for their detection. In the current work, we utilize the technique of liquid chromatography-tandem mass spectrometry (LC-MS/MS) for the determination of accumulated DNPS intermediates. The major constraint was the lack of standards. We previously developed procedures for the preparation of ADSL substrates and used them as standards in the diagnosis of ADSL deficiency via the LC-MS/MS method [3,4]. We subsequently prepared substrates of the DNPS enzymes phosphoribosylformylglycinamidine synthetase (PFAS, EC 6.3.5.3), bifunctional PAICS - phosphoribosylaminoimidazole carboxylase (EC 4.1.1.21)/phosphoribosylaminoimidazole succinocarboxamide synthetase (EC 6.3.2.6), and together with the commercially available substrate of 5-aminoimidazole-4-carboxamide ribonucleotide transformylase (EC 2.1.2.3)/inosine monophosphate cyclohydrolase (ATIC, EC 3.5.4.10), we used these substrates as the standards in the LC-MS/MS detection of DNPS defects and as substrates for the development of individual enzyme activity assays. To model the situation in the bodily fluids of patients with DNPS disorders, we prepared clustered regularly interspaced short palindromic repeats (CRISPR)-Cas9 genome-edited HeLa cells (CR-cells) deficient for specific steps of DNPS and analysed DNPS metabolites in cell lysates and growth media. We also tested the ability of the CR-cells to form purinosome, a multi-enzyme complex of DNPS enzymes, which cells transiently assemble in their cytoplasm upon depletion or an increased demand for purines [5,6].

2. Materials and methods

2.1. Chemicals and standard solutions

Succinylaminoimidazolecarboxamide ribotide (SAICAR), SAICA-riboside (SAICAr), succinyladenosine (S-Ado) and N^{10}-formyl-tetrahydrofolate (N^{10}-formyl-THF) were prepared as previously described [3,7]. Calf intestinal alkaline phosphatase (CIP) and NEB3 buffer were purchased from New England Biolabs (NEB), and Dulbecco's minimum essential medium (DMEM), F12 nutrition mix and foetal bovine serum (FBS) were obtained from Life Technologies, Thermofisher Scientific, Czech Republic. All other chemicals were purchased from Sigma-Aldrich, Czech Republic.

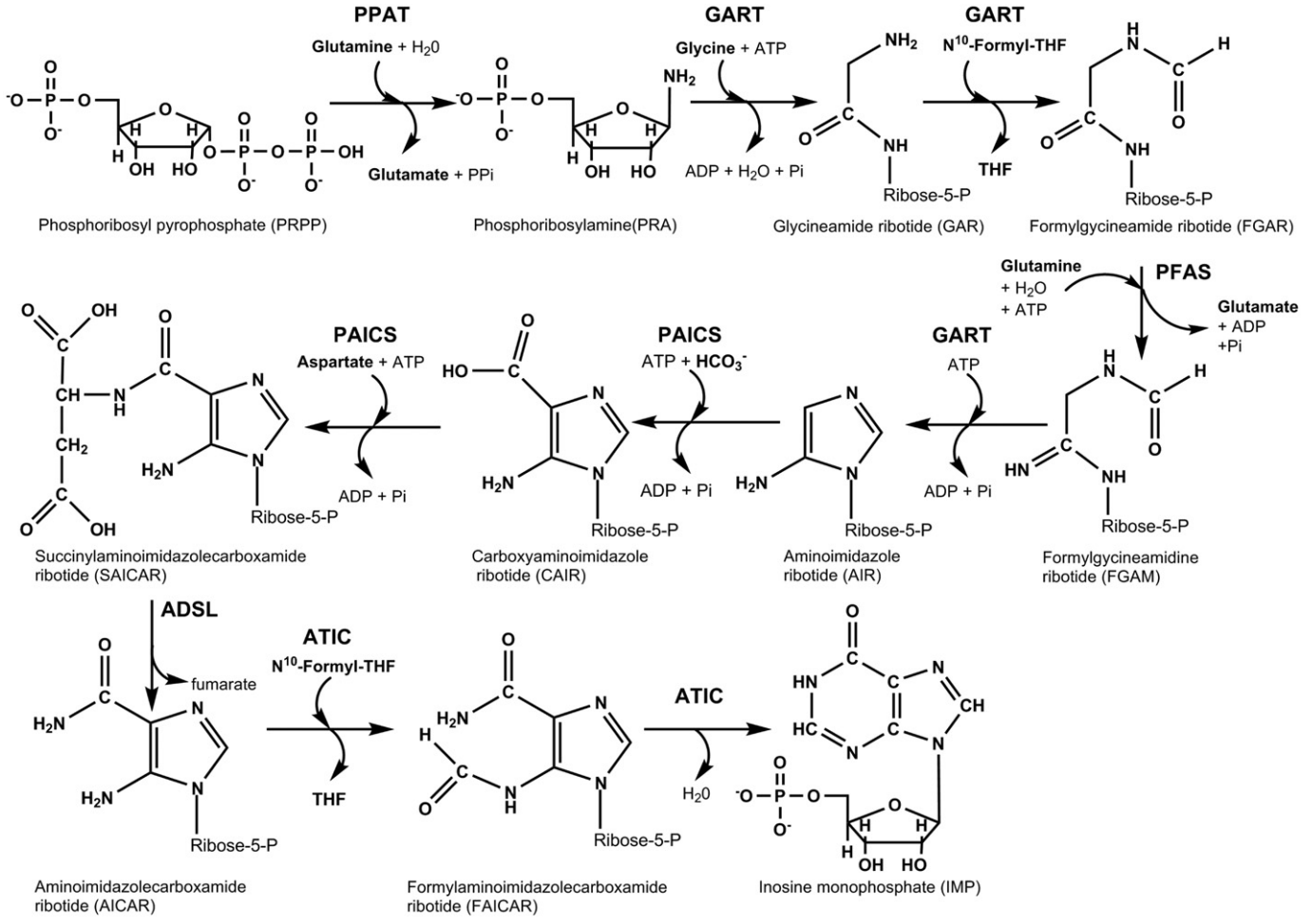

Fig. 1. De novo purine synthesis (DNPS): The basic molecule of purine inosine monophosphate (IMP) is generated within 10 reactions from organic and inorganic acids, amino acids and phosphoribosyl pyrophosphate (PRPP) using six enzymes. In the first reaction, glutamine transfers an NH_2 group to PRPP, creating a phosphoribosylamine and the side products glutamate and pyrophosphate. In subsequent reactions, other functional groups are added (from glycine, N^{10}-formyl tetrahydrofolate, glutamine, hydrogen carbon acid, aspartate and again from N^{10}-formyl tetrahydrofolate) to initiate the imidazole cycle followed by the pyrimidine cycle, the completion of which results in IMP formation.

2.2. Recombinant protein preparation

We prepared the cDNA trifunctional glycinamide ribonucleotide synthetase (EC 6.3.4.13)/aminoimidazole ribonucleotide synthetase (EC 6.3.3.1)/glycinamide ribonucleotide transformylase (EC 2.1.2.2.) (*GART*), *PFAS*, *PAICS*, *ADSL* and *ATIC* genes using previously described methods [8]. We introduced constructs with the correct sequences into the *E. coli* strain DH5αF'IQ (Invitrogen) and expressed the recombinant protein via IPTG. The pellets were resuspended in buffer A (10 mM Tris [pH 8.2], 2 mM EDTA, 10 mM KCl, 1 mM DTT, and 4% glycerol), sonicated four times for 15 s at 40 W, and centrifuged (9000*g*, 30 min); the lysates were applied to amylose affinity columns (NEB). We subsequently eluted the recombinant protein fused with maltose binding protein (MBP) from the column and performed SDS–PAGE analysis according to standard procedures.

2.3. Preparation and purification of substrates

2.3.1. Aminoimidazole ribotide (AIR) and AI-riboside (AIr)

We incubated 400 μl of a reaction mixture that contained 100 mM sodium phosphate (pH 6), 35 mM $MgCl_2$, 6 mM ADP, 6 mM SAICAR and 0.5 mg/ml human recombinant MBP-PAICS at 37 °C for 5 h and analysed the mixture via high performance liquid chromatography with diode-array detection (HPLC-DAD). We applied the reaction mixture to an activated Strata X-AW (33 μm; 200 mg/3 ml) column (Phenomenex) and immediately eluted the column using 100 mM sodium acetate pH 5.1. AIR was not captured by the column in contrast to SAICAR, ADP and ATP. We concentrated the single fractions under a stream of nitrogen and analysed them via HPLC-DAD. AIR was determined at 250 nm using a NanoDrop spectrophotometer (Thermo Scientific), and the concentration was calculated using an extinction coefficient of 3830 M^{-1} cm^{-1} [9]. We subsequently prepared AIr from the 3 mM AIR solution in the standard reaction mixture of 1xNEB3 buffer and 1 U CIP via incubation for 2 h at 37 °C.

2.3.2. Carboxyaminoimidazole ribotide (CAIR) and CAI-riboside (CAIr)

Four hundred microliters of a reaction mixture that contained 50 mM Tris-Cl (pH 8), 1.3 mM $MgCl_2$, 500 mM $NaHCO_3$, 3 mM AIR and 0.5 mg/ml human recombinant MBP-PAICS were incubated at 37 °C for 4 h and analysed via HPLC-DAD. We applied the reaction to an activated Strata XL-A (100 μm; 200 mg/3 ml) column, washed the column with 3 ml of 100 mM ammonium acetate (pH 8.2) and 3 ml of methanol and dried it under a vacuum. CAIR was eluted with 5% formic acid in methanol and analysed via HPLC-DAD. The amount of CAIR was determined at 250 nm using a NanoDrop spectrophotometer, and the concentration was calculated using an extinction coefficient of 10,580 M^{-1} cm^{-1} [9]. We subsequently prepared CAIr from the 3 mM CAIR solution in the standard reaction previously described.

2.3.3. Formylglycineamide ribotide (FGAR) and FGA-riboside (FGAr)

Four hundred microliters of a reaction mixture that contained 85 mM Tris-Cl (pH 9), 5.7 mM $MgCl_2$, 10 mM NH_4OH, 11 mM glycine, 0.7 mM ATP, 30 mM ribose-5-phosphate, 0.1 mM N^{10}-formyl-THF and 0.5 mg/ml human recombinant MBP-GART were incubated at 37 °C for 4 h and analysed via LC-MS/MS. We dephosphorylated the obtained FGAR to formylglycineamide riboside (FGAr) in the standard reaction previously described. We applied the reaction mixture to the activated column Strata X-C (33 μm; 200 mg/3 ml) and washed it with 3 ml of 0.1 N HCl. FGAr was not captured by the column in contrast to the other compounds. The FGAr fractions were concentrated under a stream of nitrogen and analysed via LC-MS/MS.

2.4. HPLC-DAD detection

The HPLC analyses were performed using a 10A Shimadzu Liquid Chromatography System with a PDA detector.

2.4.1. AIR/AIr

We applied 20 μl of the reaction mixture to a Prontosil 120–3 C18-AQ column (200 * 4 mm, 3 μm) (Bischoff Chromatography), which was subsequently eluted using a gradient initiated with 100% of phase A (0.1 M potassium phosphate buffer [pH 1.5] and 5 mM tetrabutylammonium hydrogensulfate) and 0% of phase B (phase A plus 30% of acetonitrile) at a flow rate of 0.7 ml/min. The mobile phase was adjusted linearly to 100% phase B over 0–13 min, followed by 100% B at 13–15 min and 100–0% B and 0–100% A at 15–16 min. The column was regenerated with 100% A for 19 min.

2.4.2. CAIR/CAIr

CAIR/CAIr detection was performed using the same column as the AIR detection. The gradient started with 100% of phase C (5 mM potassium dihydrogen phosphate, 75 mM dipotassium hydrogen phosphate buffer [pH 8.1] and 10 mM tetrabutylammonium bromide) and 0% of phase D (phase C plus 30% of acetonitrile) at a flow rate of 1 ml/min for 10 min. The mobile phase was adjusted linearly to 100% D and 0% C over 10–15 min, followed by 100% D at 15–17 min and 100–0% D and 0–100% C at 17–18 min. The column was regenerated with 100% C for 17 min.

2.5. CR-cell preparation

We used the GeneArt® CRISPR Nuclease Vector with an OFP Reporter Kit (Life Technologies) to knockout the genes that encoded DNPS enzymes in HeLa cells. We prepared the vectors according to the manufacturer's protocol. We transfected 5×10^6 HeLa cells using the Neon® Transfection System (Life Technologies, pulse voltage 1005 V, pulse width 35 ms, 2 pulses and 10 μl tip). The cells were seeded on 40 mm diameter Petri dishes. At 24 h post-transfection, we selected single cells positive for OFP and seeded them onto 96-well plates. We maintained the cells in DMEM with 10% FBS, 1% penicillin/streptomycin and 0.03 mM adenine. We tested the cells for protein deletion, the presence of mutations and DNPS substrate accumulation.

2.6. Mutation analysis

We isolated genomic DNA (gDNA), transcribed cDNA from the total RNA of the HeLa cells and performed PCR analysis according to standard procedures. The PCRs were conducted in 25 μl reaction mixtures that contained Red PCR Master Mix (Rovalab), 1.5 mM $MgCl_2$, 8% DMSO and 0.4 μM specific primers. We gel-purified the amplification products and sequenced the amplicons using the ABI BigDye method (Applied Biosystems).

2.7. Preparation of cell lysates

A pellet of 1×10^6 HeLa cells was dissolved in 50 μl of buffer A with Protease Inhibitor Cocktail Tablets (Roche), sonicated four times for 15 s and centrifuged at 17,000*g* for 20 min at 4 °C.

2.8. Activity assays

2.8.1. GART

The reaction was performed for 6 h at 37 °C in a 30 μl reaction mixture that contained 85 mM Tris (pH 9.0), 5.7 mM $MgCl_2$, 10 mM NH_4OH, 11.4 mM glycine, 0.7 mM ATP, 5.7 mM ribose-5-phosphate, 0.1 mM N^{10} formyl-THF and cell lysate (12.6 μg of protein). We analysed the formed FGAR/FGAr using the LC/LC-MS method.

2.8.2. PAICS

The reaction was performed for 30 min at 37 °C in a 50 μl reaction mixture that contained 50 mM Tris (pH 7.4), 13 mM $MgCl_2$, 0.45 mM ATP, 180 mM $KHCO_3$, 0.2 mM AIR and cell lysate (20 μg of protein). We measured the concentration of the formed SAICAR using the

Table 1
LC-MS/MS parameters for analytes.

Compound	Retention time (min)	MRM transitions (*m/z*)	Dwell time (ms)	DP[a] (V)	CE[b] (V)
GAr	4.51	207.1–133/73	100	35	25
FGAr	5.48	235.1–217.1/103.1/86.1	100	41	25
AIr	5.01	216.3–94/84	100	35	25
CAIr	6.89	260.2–110.0/128.2	100	35	25
SAICAr	11.31	375.2–243.0	100	35	22
AICAr	8.52	259.2–127.2/110.0	100	20	18
S-Ado	13.53	384.2–252.2	100	34	26

[a] Declustering potential.
[b] Collision energy.

HPLC-DAD method according to the previously described AIR/AIr detection procedure.

2.8.3. ADSL

The reaction was performed for 20 min at 37 °C in 50 μl of buffer A with 0.12 mM adenosine5′-(α,β-methylene) diphosphate and cell lysate (16 μg of the protein). The substrate concentrations were 0.14 and 0.09 mM for succinyladenosine monophosphate (SAMP) and SAICAR, respectively. We measured the concentrations of the formed adenosine monophosphate (AMP) and aminoimidazolecarboxamide ribotide (AICAR) using the previously described HPLC-DAD method.

2.8.4. ATIC

The reaction was performed for 1 h at 37 °C in 100 μl of solution that contained 33 mM Tris (pH 7.4), 25 mM KCl, 2.3 mM beta-mercaptoethanol, 0.1 mM N^{10}-formyl-THF, 0.5 mM AICAR and cell lysate (20 μg of protein). We analysed the concentration of the formed IMP using the previously described HPLC-DAD method.

2.9. Western blots of cell lysates

We separated the denatured protein samples via 10% SDS-PAGE and blotted them onto a PVDF membrane. The membrane was blocked with 5% BSA in PBS and probed with the following primary antibodies: mouse monoclonal anti-GART (Abnova), rabbit polyclonal anti-PFAS, mouse monoclonal anti-ATIC (Abcam), mouse monoclonal anti-PAICS (Origene) or rabbit polyclonal anti-ADSL (Atlas) diluted in 5% BSA in PBS. The target proteins were detected using species appropriate HRP labelled secondary antibodies. Chemiluminescent detection was performed using the Clarity Western ECL Substrate (Bio-Rad) and X-ray visualized.

2.10. LC-MS/MS analysis

We added 12.5 μl of 5% perchloric acid to 30 μl of the prepared lysate/medium sample, incubated for 5 min on ice, centrifuged and adjusted to pH 5–8 by the addition of 2.5 M $KHCO_3$.

The LC-MS/MS system consisted of an Agilent 1290 Infinity LC System (Agilent Technologies) coupled with an API 4000 triple quadrupole mass spectrometer with an electron ion source, which was operated using the Analyst software (Applied Biosystems).

We applied 5 μl of the sample to a Symmetry C18 column (100 * 2.1 mm, 3.5 μm, Waters Corporation). The gradient elution was initiated with 100% of A (0.1% formic acid), followed by a linear increase to 30% of B (0.1% formic acid solution in acetonitrile) over 7 min, an increase to 60% of B at 8 min and regeneration with 100% of A for 7 min. The flow rate was 0.25 ml/min. The detection of the analytes was conducted using the positive electrospray ionization technique in the reaction monitoring mode. The mass spectrometry parameters are listed in Table 1, and chromatographs are presented in Supplementary data 2.

2.11. Purinosome formation

2.11.1. Cell culture

Knockout and control HeLa cells were maintained in Dulbecco's minimum essential medium (DMEM, Gibco, Invitrogen), supplemented with 10% foetal bovine serum (FBS) (Gibco, Invitrogen) and penicillin/streptomycin (Sigma Aldrich); knockout cells were enriched with 3×10^{-5} M of adenine (purine rich (PR) medium). The purine depleted (PD) media were supplemented with dialysed 10% FBS [5] and 1% penicillin/streptomycin (Sigma Aldrich). The cells were seeded in the PR or PD medium for the immunofluorescence experiments. After 24 h, the immunofluorescence labelling was performed.

2.11.2. Immunofluorescence

The cells were fixed with 4% paraformaldehyde in PBS, permeabilized in 0.1% TRITON, blocked with 5% BSA in PBS and incubated at 4 °C overnight with the following primary antibodies: anti-rabbit polyclonal IgG anti- phosphoribosyl pyrophosphate amidotransferase (PPAT, Sigma Aldrich), mouse polyclonal IgG anti-GART (Novus Biologicals), and mouse monoclonal IgG anti-ATIC (Abcam). Species appropriate secondary antibodies, Alexa Fluor® 488 and 555 (Molecular Probes, Invitrogen), were used. Slides were mounted in ProLong® Gold Antifade

Table 2
Mutations and predicted protein changes in the CR-cells.

Cells	Edited gene	cDNA change	Predicted protein change
CR_GART1	*GART*	c.368delA	p.(Gln123Hisfs*16)
		c.367_368insA	p.(Trp124Metfs*8)
CR_GART2	*GART*	c.368delA	p.(Gln123Hisfs*16)
		c.367_368insTTGATAGAGTTCTCATGAGATCTGGTTGTCTAAAAGTGT	p.(Gln123Leufs*14)
CR_PFAS	*PFAS*	c. 2683_2684insA	p.(Thr895Asnfs*17)
		c.2683_2700insAGGCCCTCCTGGCCCCAGACTCTGTTGGACCCCCAACTCCCCCTCCAGCAGGCATCTGG + c.2684_2699delTCACTCAGGGGCTGCTGAA	p.(Thr895Lysfs*31)
CR_PAICS	*PAICS*	c.284_5insT	p.(Glu97*)
		c.285delT	p.(Ile96Metfs*8)
CR_ADSL1	*ADSL*	c.113_114insA	p.(Trp39Metfs*22)
		c.115delT	p.(Trp39Glyfs*27)
CR_ADSL2	*ADSL*	c.114_115insT	p.(Trp39Leufs*22)
		c.115_125delTGGCGGCAGCT	p.(Trp39Valfs*18)
CR_ATIC1	*ATIC*	c.81_92delTGGTTTGAATCT	p.(Gly28_Leu31del)
		Second allele is not expressed	
CR_ATIC2	*ATIC*	c. 81_91delTGGTTTGAATC	p.(Leu29Argfs*21)
		c. 81_91delTGGTTTGAATC	

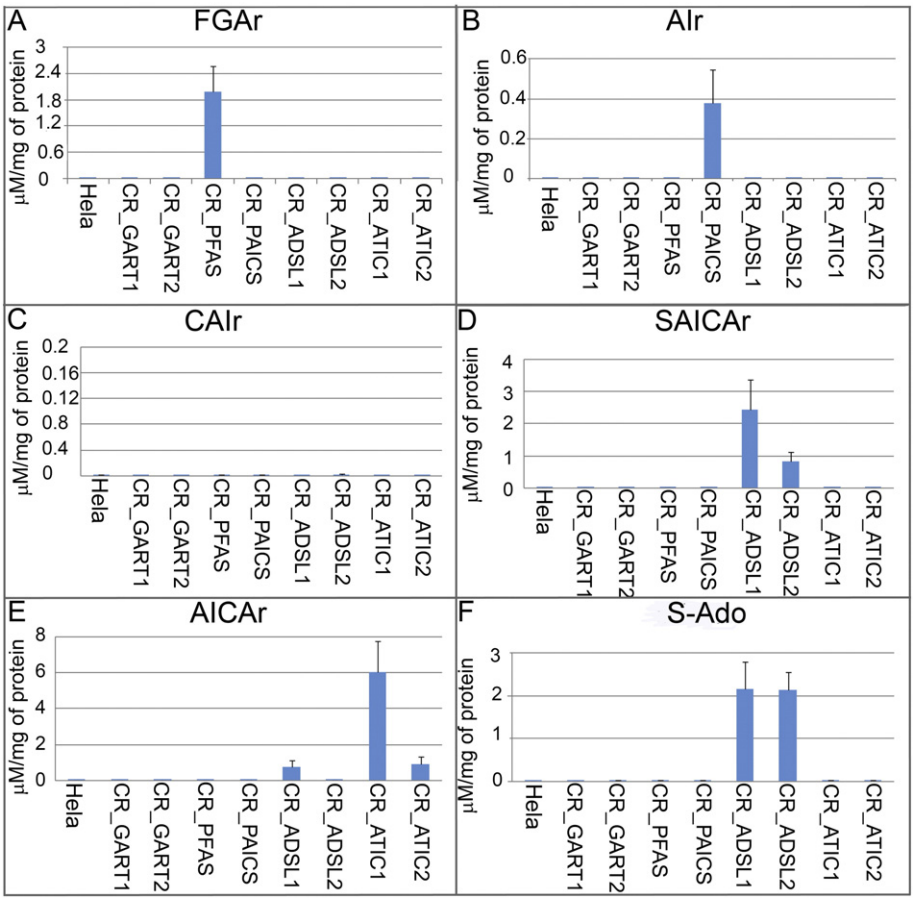

Fig. 2. Accumulation of the DNPS intermediates in HeLa cell lines deficient in specific steps of DNPS: The intermediates of the DNPS were measured by LC-MS/MS method in the cell growth media. A) FGAr was accumulated in the growth media of CR_PFAS cells. B) AIr was accumulated in the growth media of CR_PAICS cells. C) No accumulation of CAIr in growth media of any cells was observed. D) SAICAr was accumulated in the growth media of CR_ADSL cells. E) AICAr was accumulated in the growth media of CR_ATIC and in one line of CR_ADSL cells. F) S-Ado was accumulated in the growth media of CR_ADSL cells.

Mountant with DAPI (ThermoFisher Scientific). All immunofluorescence experiments were repeated at least twice.

2.11.3. Image acquisition and analysis

Prepared slides were analysed via confocal microscopy. XYZ images were sampled according to the Nyquist criterion using a LeicaSP8X confocal microscope, HC PL APO OIL CS2 objective (60×, N.A.1.40), and 470–670 nm 80 MHz pulse continuum WLL2 (488 and 543 laser lines). Images were restored using a classic maximum likelihood restoration algorithm in Huygens Professional Software (SVI). The colocalization maps, which employed single pixel overlap coefficient values that ranged from 0 to 1, were created in Huygens Professional Software. The resulting overlap coefficient values are presented as pseudocolors, and the scale is shown in the corresponding lookup tables (LUT).

3. Results

3.1. Preparation and purification of DNPS intermediates

The strategies used for substrate production were based on the preparation of the human recombinant enzymes MBP-GART and MBP-PAICS.

The PAICS metabolite AIR was converted from SAICAR in an enzymatic reaction with MBP-PAICS and purified on a weak anion-exchange functionalized polymeric sorbent with a production yield of 22%. The purity of the prepared metabolite determined by HPLC-DAD analysis was 84%. In the second reaction, we dephosphorylated the resulting AIR to AIr via CIP.

CAIR was produced from AIR in a forward reaction catalysed by MBP-PAICS and purified on a strong anion-exchange polymeric sorbent. CAIR was contaminated by AIR, and the purity determined by HPLC-DAD was 60%. The resulting CAIR was dephosphorylated to CAIr by CIP.

The PFAS substrate, FGAR, is the resulting product of three reactions that occurred in one step. The first reaction is the formation of 5-phosphoribosylamine (PRA) from ribose-5-phosphate and ammonium hydroxide as a function of the pH [10]. In the second and third enzymatic reactions, PRA is converted by MBP-GART to form FGAR via the intermediate glycineamide ribotide. Due to FGAR instability, we immediately dephosphorylated FGAR to FGAr via CIP and purified the product on a strong cation-exchange polymeric sorbent.

3.2. Preparation of HeLa cells deficient for specific steps of DNPS

We knocked out genes that coded DNPS enzymes in HeLa cells using the CRISPR-Cas9 genome editing system. We detected positive clones via cDNA and gDNA sequencing, western blot analysis, LC-MS/MS and activity assays, if available. We prepared cell lines with knocked-out *GART*, *PFAS*, *PAICS*, *ADSL* and *ATIC*. All mutations in the targeted genes comprised insertions or deletions of at least one nucleotide, which resulted in a disrupted reading frame (Table 2) and no detectable protein expression.

3.3. Determination of DNPS metabolites in HeLa cells deficient for specific steps of DNPS

3.3.1. Linearity, limits of detection (LOD) and quantification (LOQ)

We confirmed the linearity of the method via the generation of linear calibration curves with high correlation coefficients ($r > 0.9911$) in the range of the indicated concentrations.

The LOD and LOQ were defined using signal-to-noise ratios of 3:1 and 10:1, respectively. The LOD and LOQ values were determined to be 0.0094 and 0.031 μmol/l, respectively, for FGAr, 0.048 and 0.16 μmol/l, respectively, for AIr, 0.077 and 0.25 μmol/l, respectively, for CAIr, 0.0023 and 0.0076 μmol/l, respectively, for AICAriboside (AICAr), 0.019 and 0.063 μmol/l, respectively, for SAICAr and 0.014 and 0.0046 μmol/l, respectively, for S-Ado.

3.3.2. DNPS metabolites in CR-cell lysates and growth media

We analysed the metabolites in the CR-cell lysates and growth media using the LC-MS/MS method with DNPS intermediate inner standards. We detected increased levels of FGAr in the growth medium of the PFAS-deficient cells (CR_PFAS, Fig. 2A), increased levels of AIr in the growth medium of the PAICS-deficient cells (CR_PAICS, Fig. 2B), increased levels of SAICAr (Fig. 2D) and S-Ado (Fig. 2F) in the growth medium of the ADSL-deficient cells (CR_ADSL), in the growth medium of CR_ADSL1 cells was further observed slightly increased level of AICAr (Fig. 2E) and increased levels of AICAr (Fig. 2E) and SAICAr (Fig. 2D) in the growth medium of the ATIC-deficient cells (CR_ATIC). We did not detect CAIr (Fig. 2C) or the GAr metabolite (data not shown) in the cell media or lysates. No metabolite of DNPS was identified in the cell lysates.

3.4. Activity assays

The enzyme activity was measured by HPLC in the CR_PFAS, CR_PAICS, CR_ADSL, CR_ATIC and control cell lysates. The protein activity measured in the control cells was set to 100%, and the activity of specific proteins in the CR-cells was set to relative numbers to the controls. We did not identify activity of the knockout protein in the CR_PFAS, CR_PAICS or CR_ATIC cells, and in the CR_ADSL cells, the activity decreased to 2.6 ± 3% of the control cells (Fig. 3A).

3.5. Western blots

To determine the ability of the CR-cells to process the proteins, we performed Western blot analyses of the cell lysates. The CR-cells did not produce a specific knockout protein (Fig. 3B).

3.6. Purinosome formation

To determine whether the mutations of the *GART*, *PFAS*, *PAICS*, *ADSL* and *ATIC* genes affect the intracellular compartmentalization of DNPS proteins in vivo, we investigated purinosome formation in CR-cells. To detect purinosome formation, we cultured Hela cells in PD and PR media, and we immuno-labelled the combination of PPAT and ATIC in the CR_GART cells and PPAT and GART in the remaining cells.

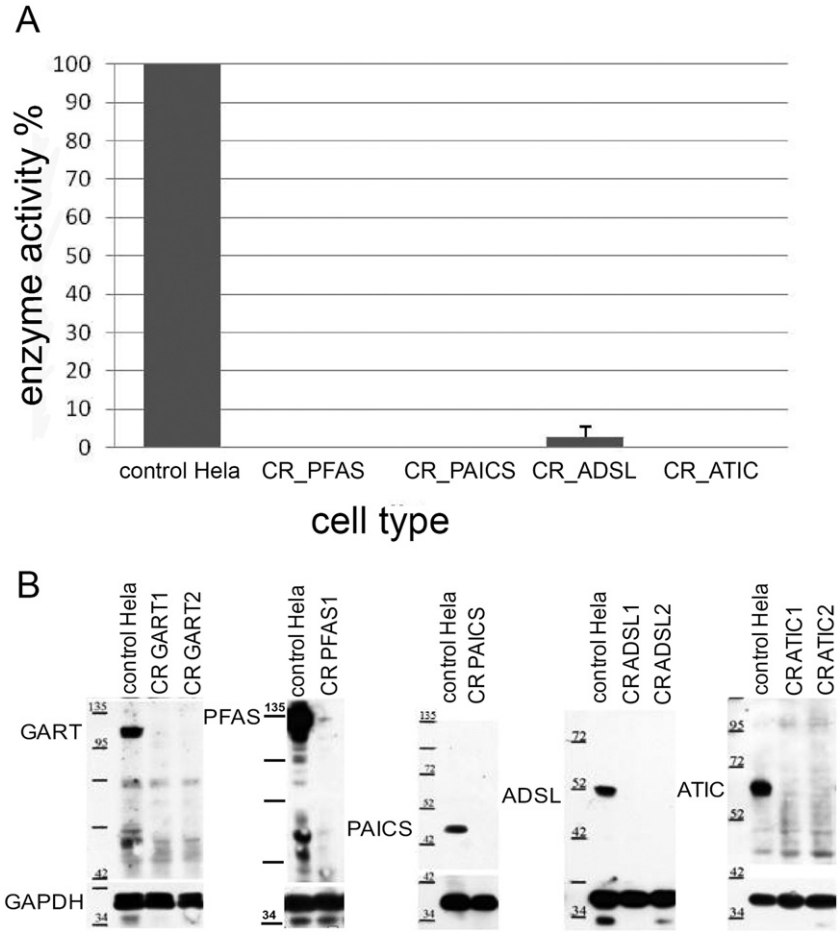

Fig. 3. Characterization of the CR-cells: A) Activity assays: The activity of GART, PFAS, ADSL and ATIC in control Hela cells was set as 100%. Compared to controls CR_GART cells have 0% activity of GART, CR_PFAS have 0% activity of PFAS, CR_ADSL have 1,7% activity of ADSL and CR_ATIC have 0% activity of ATIC. B) Western blot analysis of DNPS proteins in cell lysates demonstrating absence of GART, PFAS, PAICS, ADSL or ATIC in the knockout cells.

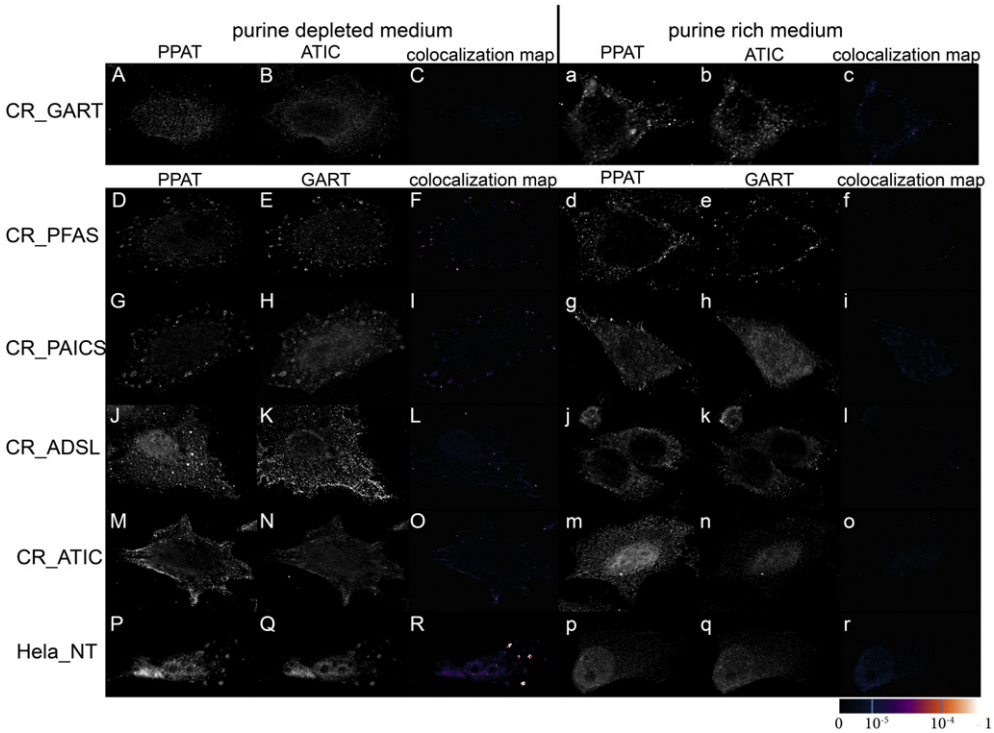

Fig. 4. Purinosome formation: The purinosome formation in the purine depleted medium was disrupted in cell lines where GART (A, B, C), ADSL (J, K, L) and bifunctional enzyme ATIC (M, N, O) were knocked-out. In cell lines with the knockout of PFAS (D, E, F) and PAICS (G, H, I) was the purinosome formation reduced when compared to control Hela cells (P, Q, R). In the purine rich medium the proteins remained diffuse and did not colocalize (a–r). Colocalization maps (C, F, I, L, O, R; c, f, i, l, o, r) display the values of the coefficients of the fluorescent signals overlaps. The values are transformed into pseudocolor which scale is shown at right bottom in corresponding LUT.

In the CR_GART (Fig. 4A, B, C), CR_ADSL (Fig. 4J, K, L) and CR_ATIC (Fig. 4M, N, O) cells grown in the PD medium, there was no granular staining of the immunolabelled proteins with no signal overlaps (Fig. 4C, L, O), which suggests the disruption of purinosome formation. In the CR_ PFAS (Fig. 4D, E, F) and CR_PAICS (Fig. 4G, H, I) cell lines grown in the PD medium, there was fine granular staining, and the image analysis indicated very low signal overlaps (Fig. 4F, I), which suggests highly reduced purinosome formation compared with the control Hela cells (Fig. 4P, Q, R). Regarding the cells grown in the PR medium, the proteins remained diffuse and did not exhibit colocalization (Fig. 4a–r). The colocalization maps (Fig. 4C, F, I, L, O, R; c, f, i, l, o, r) indicate the values of the coefficients of the fluorescent signal overlaps.

4. Discussion

As a result of the low incidence of known DNPS disorders, including 80 published cases of ADSL deficiency [11] and one case of AICA-ribosiduria worldwide [2], these diseases are most likely under-diagnosed. Patients with DNPS disorders are disadvantaged because of the broad, unspecific neurological symptoms; therefore, screening for known DNPS metabolic disorders is delayed. In cases with a severe phenotype, which typically end with early death, the diseases remain undiagnosed. Prenatal diagnosis in a subsequent pregnancy is therefore excluded.

Furthermore, specialized laboratory screening for metabolic disorders may not produce satisfactory results because of the limits of the diagnostic methods. Thus, laboratories primarily focus on ADSL deficiency and rarely on AICA-ribosiduria. To date, no other genetically determined defects of the DNPS have been described; however, the existence of defects is highly likely.

In the current study, we prepared individual recombinant enzymes of the DNPS pathway and used them in the biochemical preparation of the commercially unavailable enzyme substrates. These compounds were used in parallel as standards for the development and validation of their quantitative LC-MS/MS detection, as well as substrates for the development of enzyme activity assays.

We subsequently prepared CRISPR-Cas9 genome-edited HeLa cells deficient for specific steps of DNPS to demonstrate the potential situation in the bodily fluids of patients with genetically determined defects of the DNPS enzymes. It is a first human cellular model of all possible genetically determined defects of DNPS. Previously there were described and characterized models of Chinese hamster ovary (CHO) cells defected in PAICS and ADSL enzymes. The authors detected the accumulation of AIR in lysates of PAICS defected CHO cells. The accumulation of SAICAR, SAMP and in presence of SAICAR in growth media AIR was detected in lysates of ADSL deficient CHO cells [12,13]. In contrast to our findings, the DNPS intermediates were undetectable by LC-MS/MS in cell lysates of all prepared human model CR-cells. However, we identified an accumulation of the dephosphorylated substrate(s) for the defective enzyme in the growth media of model cells, with the exception of the cells with defective GART enzyme. This finding is a result of the instability of the GART substrate phosphoribosylamine, which has a half-life of 5 s under physiological conditions and is hydrolysed to ribose 5-phosphate, an intermediate of the pentose phosphate pathway [14]. Furthermore, we have unexpectedly detected, together with dephosphorylated ADSL substrates, dephosphorylated enzyme product AICAr in the CR_ADSL1 cells. AICAR crossroads between two metabolic pathways - DNPS and histidine metabolism. After the blockage of the ADSL reaction, a significant amount of AICAR can be provided through the alternative pathway [15]. Thus the accumulation of the AICAr in the growth media of CR_ADSL1 cells may be a result of the regulatory crosstalk between these two pathways.

We did not analyze substrates of affected enzymes such as amino acids, N^{10}-formyl-THF and bicarbonate considering their role in multiple pathways in organism. Therefore, we did not expect a measurable increase in their concentration.

Finally, using fluorescence microscopy, we determined that each of the DNPS enzyme deficiencies disrupted the formation of the purinosome in CR_cells. It is in accordance with previously published results that the

purinosome formation in ADSL deficient and AICAribusiduria fibroblasts is fully dependent on the presence of structurally intact ATIC and ADSL protein complexes and presumably also on the presence of all the other DNPS proteins [6]. CR_cells with mutated DNPS genes resulting in no detectable DNPS protein expression can serve as useful human model systems for the analysis of purinosome assembly and function. The study of purinosome formation by the endogenous proteins immunodetection in previously prepared CHO cells [12,13] has failed due to the unavailability of functional primary antibodies against hamster proteins (unpublished results).

5. Conclusion

We conclude that LC-MS/MS analysis of the dephosphorylated substrates of PFAS, PAICS, ADSL and ATIC enzymes in bodily fluids, such as urine, plasma and cerebrospinal fluid, is applicable in the selective screening of known and putative DNPS disorders. Similar to known disorders ADSL deficiency and AICA-ribosiduria, which are manifested by accumulation of metabolites SAICAr and S-Ado, or AICAr, respectively, in the bodily fluids of patients, the putative genetically determined defects of the enzymes PFAS and PAICS will manifest by the accumulation of their dephosphorylated substrates FGAr or AIr, respectively. Moreover, this approach should be considered in patients with neurological and neuromuscular diseases of unknown aetiology. In the case of positive results, a molecular biological examination of individual genes may follow, and genetic counselling may be established.

Human cellular models of HeLa cells deficient in particular steps of DNPS provide important insights about the pathogenesis of DNPS disorders and represent an interesting way for the screening of potential therapeutic agents. Furthermore, these cellular models offer advantages in various studies that investigate the mechanisms of purinosome formation and regulation.

Acknowledgements

The authors acknowledge Prof. Tomas Adam for providing us with control FGAr.

This work was supported by from the Ministry of Health of the Czech Republic [grant AZV 15-28979A] and by the Charles University in Prague [grant GAUK 818416]. Institutional support was provided by the Charles University in Prague [programs UNCE 204011, PRVOUK-P24/LF1/3 and SVV UK 260256/2016], by the Ministry of Education, Youth and Sports of CR [LQ1604 National Sustainability Program II], by the project "BIOCEV" [CZ.1.05/1.1.00/02.0109], by OP Prague Competitiveness [project CZ.2.16/3.1.00/24012].

Appendix A. Supplementary data

Supplementary data to this article can be found online at http://dx.doi.org/10.1016/j.ymgme.2016.08.004.

References

[1] G. Van den Berghe, J. Jaeken, Adenylosuccinase deficiency, Adv. Exp. Med. Biol. 195 (1986) 27–33.
[2] S. Marie, B. Heron, P. Bitoun, T. Timmerman, G. Van Den Berghe, M.F. Vincent, AICA-ribosiduria: a novel, neurologically devastating inborn error of purine biosynthesis caused by mutation of ATIC, Am. J. Hum. Genet. 74 (2004) 1276–1281.
[3] M. Zikanova, J. Krijt, H. Hartmannova, S. Kmoch, Preparation of 5-amino-4-imidazole-N-succinocarboxamide ribotide, 5-amino-4-imidazole-N-succinocarboxamide riboside and succinyladenosine, compounds usable in diagnosis and research of adenylosuccinate lyase deficiency, J. Inherit. Metab. Dis. 28 (2005) 493–499.
[4] M. Zikanova, J. Krijt, V. Skopova, M. Krijt, V. Baresova, S. Kmoch, Screening for adenylosuccinate lyase deficiency using tandem mass spectrometry analysis of succinylpurines in neonatal dried blood spots, Clin. Biochem. 48 (2015) 2–7.
[5] S. An, R. Kumar, E.D. Sheets, S.J. Benkovic, Reversible compartmentalization of de novo purine biosynthetic complexes in living cells, Science 320 (2008) 103–106.
[6] V. Baresova, V. Skopova, J. Sikora, D. Patterson, J. Sovova, M. Zikanova, S. Kmoch, Mutations of ATIC and ADSL affect purinosome assembly in cultured skin fibroblasts from patients with AICA-ribosiduria and ADSL deficiency, Hum. Mol. Genet. 21 (2012) 1534–1543.
[7] P.B. Rowe, A simple method for the synthesis of N5,N10-methenyltetrahydrofolic acid, Anal. Biochem. 22 (1968) 166–168.
[8] S. Kmoch, H. Hartmannova, B. Stiburkova, J. Krijt, M. Zikanova, I. Sebesta, Human adenylosuccinate lyase (ADSL), cloning and characterization of full-length cDNA and its isoform, gene structure and molecular basis for ADSL deficiency in six patients, Hum. Mol. Genet. 9 (2000) 1501–1513.
[9] E. Meyer, N.J. Leonard, B. Bhat, J. Stubbe, J.M. Smith, Purification and characterization of the purE, purK, and purC gene products: identification of a previously unrecognized energy requirement in the purine biosynthetic pathway, Biochemistry 31 (1992) 5022–5032.
[10] D.P. Nierlich, B. Magasanik, Phosphoribosylglycinamide synthetase of aerobacter aerogenes. purification and properties, and nonenzymatic formation of its substrate 5′-phosphoribosylamine, J. Biol. Chem. 240 (1965) 366–374.
[11] A. Jurecka, M. Zikanova, S. Kmoch, A. Tylki-Szymanska, Adenylosuccinate lyase deficiency, J. Inherit. Metab. Dis. 38 (2015) 231–242.
[12] N. Duval, K. Luhrs, T.G. Wilkinson 2nd, V. Baresova, V. Skopova, S. Kmoch, G.N. Vacano, M. Zikanova, D. Patterson, Genetic and metabolomic analysis of AdeD and AdeI mutants of de novo purine biosynthesis: cellular models of de novo purine biosynthesis deficiency disorders, Mol. Genet. Metab. 108 (2013) 178–189.
[13] L.K. Vliet, T.G. Wilkinson 2nd, N. Duval, G. Vacano, C. Graham, M. Zikanova, V. Skopova, V. Baresova, A. Hnizda, S. Kmoch, D. Patterson, Molecular characterization of the AdeI mutant of Chinese hamster ovary cells: a cellular model of adenylosuccinate lyase deficiency, Mol. Genet. Metab. 102 (2011) 61–68.
[14] J. Rudolph, J. Stubbe, Investigation of the mechanism of phosphoribosylamine transfer from glutamine phosphoribosylpyrophosphate amidotransferase to glycinamide ribonucleotide synthetase, Biochemistry 34 (1995) 2241–2250.
[15] K. Rebora, B. Laloo, B. Daignan-Fornier, Revisiting purine-histidine cross-pathway regulation in *Saccharomyces cerevisiae*: a central role for a small molecule, Genetics 170 (2005) 61–70.